J. ADV. SIMULAT. SCI. ENG.
Vol. 6, No. 1, 11-20.

Computation of non-isothermal and compressible low Mach number gas flows by fully explicit scheme using control method for speed of sound

Daisuke Toriu[1,*] and Satoru Ushijima[1]

[1]Academic Center for Computing and Media Studies (ACCMS), Kyoto University

[*]toriu.daisuke.8v@kyoto-u.ac.jp

Received: October 30, 2018; Accepted: January 3, 2019; Published: March 15, 2019

Abstract. In this study, we propose a new fully explicit scheme for non-isothermal and compressible low Mach number gas flows based on a fractional step method and a control method for the speed of sound. Since the Courant-Friedrichs-Lewy (CFL) condition based on the speed of sound is improved according to an artificial coefficient for pressure fluctuation terms, the time increment in the proposed method can be set on the same order as that of a conventional semi-implicit method which treats pressure terms in momentum and energy equations implicitly. As a result of the application to the natural convection in a square cavity, it is demonstrated that the proposed fully explicit method enables to conduct computations reasonably about $6 \sim 8$ times faster than the conventional semi-implicit method by setting the appropriate value of the artificial coefficient for pressure fluctuation terms.

Keywords: Fully explicit scheme, Speed of sound, Non-isothermal flow, Compressible low Mach number flow

1. Introduction

In our previous study [1], a semi-implicit fractional step method for non-isothermal and compressible low Mach number gas flows was proposed to calculate thermal interactions between fluids and solid objects under high temperature difference conditions. In this method, advection and diffusion terms in governing equations written in the conservative form are treated explicitly. By contrast, pressure terms in momentum and energy equations are treated implicitly based on the temperature-based CIP-CUP (TCUP) method [2] to improve the Courant-Friedrichs-Lewy (CFL) condition based on the speed of sound. As a result, our conventional semi-implicit method enables to calculate compressible low Mach number flows using the time increment comparable to that in incompressible flow solvers.

However, it is considered that the computational stage of simultaneous linear equations becomes a bottleneck of performance in future large-scale parallel computations.

As other methods to calculate compressible low Mach number flows efficiently, the preconditioning method [3, 4] and the reduced speed of sound technique [5, 6] were proposed in previous studies. In these methods, the speed of sound can be controlled artificially, and the CFL condition based on it is improved without using implicit treatment of pressure terms in momentum and energy equations. Especially, the reduced speed of sound technique [5, 6] enables to control the speed of sound simply by using an artificial coefficient in the advection term on the mass conservation equation. However, the conventional reduced speed of sound technique [5, 6] cannot be applied directly to our original fractional step method [1] since the conventional technique is proposed for the compressive magnetohydrodynamics equations and numerical procedures are different from those of our method.

On the basis of such background, we propose a new control method for the speed of sound which can be applied to our original fractional step method for non-isothermal and compressible low Mach number flows in this study. In addition, the applicability of a new fully explicit scheme using the proposed method is confirmed through computations of natural convection in a square cavity.

2. Numerical method

2.1. Governing equations

In this study, governing equations of the compressible fluid are given by following mass conservation, momentum, and energy equations:

$$\frac{\partial \rho}{\partial t} + \frac{\partial (\rho u_j)}{\partial x_j} = 0, \tag{1}$$

$$\frac{\partial (\rho u_i)}{\partial t} + \frac{\partial (\rho u_i u_j)}{\partial x_j} = -\frac{\partial p'}{\partial x_i} + \frac{\partial \tau_{ij}}{\partial x_j} + \rho f_i, \tag{2}$$

$$\frac{\partial (\rho e)}{\partial t} + \frac{\partial (\rho e u_j)}{\partial x_j} = -p' \frac{\partial u_i}{\partial x_i} + \tau_{ij} \frac{\partial u_i}{\partial x_j} - \frac{\partial q_i}{\partial x_i}, \tag{3}$$

where t is the time and x_i is the component of orthogonal coordinates, respectively. In addition, ρ is the density, u_i is the velocity, p' is the approximated pressure which enables us to control the speed of sound, τ_{ij} is the viscous stress, f_i is the external force, e is the internal energy, and q_i is the heat flux, respectively. The fluid is assumed to be the Newtonian fluid and the Fourier's law is adopted in this study. Thus, τ_{ij} and q_i are given by as follows:

$$\tau_{ij} = \mu \left(\frac{\partial u_i}{\partial x_j} + \frac{\partial u_j}{\partial x_i} \right) - \frac{2}{3} \mu \frac{\partial u_m}{\partial x_m} \delta_{ij}, \tag{4}$$

$$q_i = -\lambda \frac{\partial T}{\partial x_i}, \tag{5}$$

where μ is the coefficient of viscosity, δ_{ij} is the Kronecker delta, λ is the thermal conductivity, and T is the temperature, respectively. In addition, the fluid is assumed to be the ideal

gas and the equation relating e and T is

$$e = C_V T, \tag{6}$$

where C_V is the specific heat at constant volume.

As given by Eqs. (2) and (3), the approximated pressure p' is used in the right-hand side of momentum and energy equations to control the speed of sound. On the other hand, the actual pressure p is given by the following equation of state for the ideal gas:

$$p = (\gamma - 1)\rho e, \tag{7}$$

where γ is the specific heat ratio. In the derivation process of p', p is rewritten with the fluctuation $\tilde{p}$ from the initial pressure as follows:

$$p = p_0 + \tilde{p} = p_0 + \alpha\tilde{p} + (1 - \alpha)\tilde{p}, \tag{8}$$

where p_0 is the initial pressure and α is a constant value which satisfies $0 < \alpha \leq 1$. In this study, we approximate $\tilde{p}$ in the third term on the right-hand side of Eq. (8) by $\bar{P}$ which is the spatially averaged value of $\tilde{p}$. As a result of this approximation, p' is defined as

$$p' \equiv p_0 + \alpha\tilde{p} + (1 - \alpha)\bar{P}. \tag{9}$$

By using p' in momentum and energy equations, we can obtain the propagation equation of $\tilde{p}$ in isentropic flows and in the very short time period from the initial state as follows:

$$\frac{\partial^2 \tilde{p}}{\partial t^2} = \alpha A_0^2 \frac{\partial^2 \tilde{p}}{\partial x_i^2}, \tag{10}$$

where A_0 is the speed of sound given by $A_0 = \sqrt{(\gamma p_0)/\rho_0}$ and ρ_0 is the initial density. Equation (10) represents that the speed of sound decreases to $\sqrt{\alpha}A_0$ $(0 < \alpha \leq 1)$. Thus, the larger time increment can be adopted in our method since the CFL condition based on the speed of sound is improved depending on the value of α as follows:

$$\Delta t < \frac{\Delta x}{\sqrt{\alpha}A_0} \quad (0 < \alpha \leq 1), \tag{11}$$

where Δt and Δx are the time increment and the size of a computational cell.

2.2. Numerical procedure

The numerical procedure of the proposed fully explicit method is divided into three stages [1], advection, diffusion, and acoustic stages. The governing equations in each computational stage are discretized on the collocated grid system [7] and variables are updated

fractionally. In the advection stage, advection terms in Eqs. (1), (2), and (3) are considered as follows:

$$\left.\frac{\partial \rho}{\partial t}\right|_{\mathrm{Adv}} + \frac{\partial(\rho u_j)}{\partial x_j} = 0, \tag{12}$$

$$\left.\frac{\partial(\rho u_i)}{\partial t}\right|_{\mathrm{Adv}} + \frac{\partial(\rho u_i u_j)}{\partial x_j} = 0, \tag{13}$$

$$\left.\frac{\partial(\rho e)}{\partial t}\right|_{\mathrm{Adv}} + \frac{\partial(\rho e u_j)}{\partial x_j} = 0. \tag{14}$$

Equations (12), (13), and (14) are solved explicitly based on the finite volume method and the third order MUSCL-TVD scheme [8].

The governing equations for the diffusion stage are given by

$$\left.\frac{\partial \rho}{\partial t}\right|_{\mathrm{Diff}} = 0, \tag{15}$$

$$\left.\frac{\partial(\rho u_i)}{\partial t}\right|_{\mathrm{Diff}} = \frac{\partial \tau_{ij}}{\partial x_j}, \tag{16}$$

$$\left.\frac{\partial(\rho e)}{\partial t}\right|_{\mathrm{Diff}} = \tau_{ij}\frac{\partial u_i}{\partial x_j} - \frac{\partial q_i}{\partial x_i}. \tag{17}$$

Equations (16) and (17) for viscous and heat flux terms are solved explicitly based on the TCUP method [2]. In addition, $\tilde{p}$ and p' are updated considering variations of ρ and e in advection and diffusion stages as follows:

$$\begin{aligned}
\tilde{p}^{**} &= p^{**} - p_0 = (\gamma-1)\rho^{**}e^{**} - p_0 \\
&= (\gamma-1)(\rho_0 + \tilde{\rho}^{**})(e_0 + \tilde{e}^{**}) - p_0 \\
&= (\gamma-1)(\rho_0\tilde{e}^{**} + \tilde{\rho}^{**}e_0 + \tilde{\rho}^{**}\tilde{e}^{**}) + (\gamma-1)\rho_0 e_0 - p_0 \\
&= (\gamma-1)(\rho_0\tilde{e}^{**} + \tilde{\rho}^{**}e_0 + \tilde{\rho}^{**}\tilde{e}^{**}),
\end{aligned} \tag{18}$$

$$p'^{**} = p_0 + \alpha\tilde{p}^{**} + (1-\alpha)\bar{P}^{**}, \tag{19}$$

where the superscript $**$ represents the variable after the diffusion stage and the subscript 0 represents the initial value of each variable. In addition, $\tilde{\rho}$ and $\tilde{e}$ are fluctuations of the density and the internal energy from each initial value.

In the final computational stage, acoustic stage, pressure and external force terms are considered as follows:

$$\left.\frac{\partial \rho}{\partial t}\right|_{\mathrm{Acous}} = 0, \tag{20}$$

$$\left.\frac{\partial(\rho u_i)}{\partial t}\right|_{\mathrm{Acous}} = -\frac{\partial p'}{\partial x_i} + \rho f_i, \tag{21}$$

$$\left.\frac{\partial(\rho e)}{\partial t}\right|_{\mathrm{Acous}} = -p'\frac{\partial u_i}{\partial x_i}. \tag{22}$$

In our conventional semi-implicit method [1], the pressure terms of the momentum and energy equations are treated implicitly in the acoustic stage to improve the CFL condition based on the speed of sound. By contrast, p' is adopted in this study, and the next time step velocity u_i^{n+1} and pressure p'^{n+1} are calculated explicitly as follows:

$$u_i^{n+1} = u_i^{**} + \Delta t\left(-\frac{1}{\rho^{**}}\frac{\partial p'^{**}}{\partial x_i} + f_i\right), \tag{23}$$

$$p'^{n+1} = p'^{**} - \alpha\Delta t(1-\gamma)p'^{**}\frac{\partial u_i^{n+1}}{\partial x_i}. \tag{24}$$

By updating u_i^{n+1} and p'^{n+1} as given by Eqs. (23) and (24), the proposed method enables to calculate compressible low Mach number flows efficiently without solving the simultaneous linear equations.

3. Results and discussion

The proposed method is applied to the natural convection in a 2-dimensional square cavity using 1 core of the supercomputer system in Kyoto University (CRAY CS400 2820XT, Intel Xeon Broadwell 18cores 2.1GHz × 2 / node). Figure 1 shows the computational area. In this application, the left-hand side wall is heated at T_h, and the right-hand side wall is cooled at T_c. In addition, adiabatic conditions are imposed on top and bottom walls. The Prandtl number and the specific heat ratio of the fluid are fixed at $Pr = 0.71$ and $\gamma = 1.40$ by assuming that the fluid is air and the maximum temperature change is about 100 [K]. Actually, Pr and γ of the air change only about 0.4% between 300 to 400 [K] [9], which is our target temperature range in this study. The two different Rayleigh numbers Ra are considered, namely, $Ra = 10^3$ and 10^6. For $Ra = 10^3$, ΔT is 1.0 [K] and $\beta\Delta T$ is 3.33×10^{-3} ($<< 1$). Here, β and ΔT are the coefficient of volume expansion of the fluid and the temperature difference between heated and cooled walls, respectively. By contrast, ΔT is 100 [K] and $\beta\Delta T$ is 0.33 in the case for $Ra = 10^6$ to consider the influence of the fluid compressibility. In addition, the different numbers of computational cells are set in each Ra condition, namely, 100×100 for $Ra = 10^3$ and 150×150 for $Ra = 10^6$.

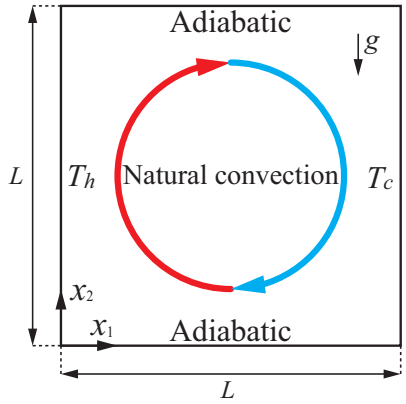

Figure 1: Computational area of natural convection in a square cavity

The computations are conducted using different values of α as given by Table 1. The maximum allowable time increment is set in each α condition, and obtained maximum Courant numbers $C_{a,\max}$ based on the speed of sound in the steady state are given in Table 1. Here, the Courant number C_a is calculated as follows:

$$C_a = \max\left\{\frac{|u_1| + A}{\Delta x_1}\Delta t,\ \frac{|u_2| + A}{\Delta x_2}\Delta t\right\}, \tag{25}$$

where Δx_1 and Δx_2 are computational cell sizes in x_1 and x_2 directions, respectively.

The predicted time histories of isotherms for $Ra = 10^3$ and 10^6 are shown in Figs. 2 and 3. Here, both results are obtained by using maximum α values in each Ra condition ($\alpha = 10^{-5}$ for $Ra = 10^3$ and $\alpha = 5.0 \times 10^{-5}$ for $Ra = 10^6$). In addition, t' is the non-

Table 1: $C_{a,\max}$ in steady state

$Ra = 10^3$	α	1.0	0.50	0.10	1.0×10^{-3}	5.0×10^{-5}	1.0×10^{-5}
	$C_{a,\max}$	1.06	1.55	3.51	33.4	1.55×10^2	3.34×10^2
$Ra = 10^6$	α	1.0	0.50	0.10	1.0×10^{-3}	5.0×10^{-5}	1.0×10^{-5}
	$C_{a,\max}$	1.13	1.57	3.58	35.8	1.57×10^2	–

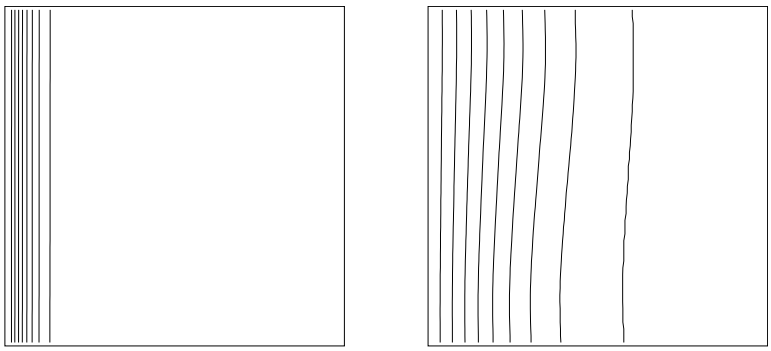

(a) $t' = 3.81 \times 10^{-3}$ (b) $t' = 3.81 \times 10^{-2}$

(c) $t' = 7.61 \times 10^{-2}$ (d) steady state

Figure 2: Time history of isotherms ($Ra = 10^3$, $\alpha = 10^{-5}$)

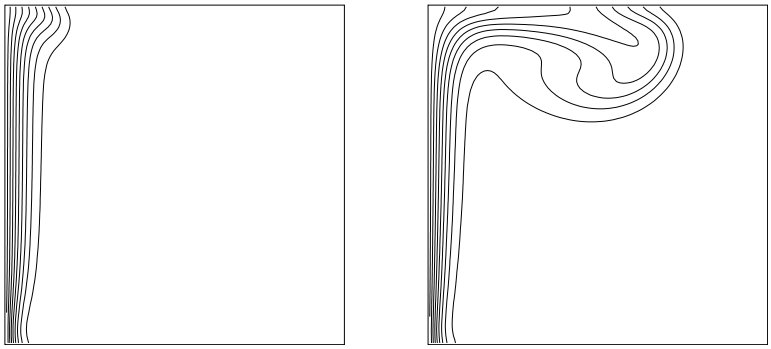

(a) $t' = 9.00 \times 10^{-4}$ (b) $t' = 2.16 \times 10^{-3}$

(c) $t' = 5.40 \times 10^{-3}$ (d) steady state

Figure 3: Time history of isotherms ($Ra = 10^6$, $\alpha = 5.0 \times 10^{-5}$)

dimensional time defined as $t' = t\kappa/L^2$ where κ is the thermal diffusivity and L is the length of the computational area. As shown in Figs. 2 and 3, the natural convection is developed in the computational area and the steady state is calculated stably using the control method for the speed of sound. In addition, Table 2 gives the comparison of the predicted minimum fluid density in the steady state. Here, $\rho_{f,\min}$ is the minimum value of the fluid density in the steady state and $\rho_{f,0}$ is the spatial averaged value of the fluid density in the initial state ($t' = 0.0$). In the case for $Ra = 10^3$ and $\beta\Delta T = 3.33 \times 10^{-3}$, the change of the fluid density is negligible since $\beta\Delta T$ is sufficiently small. By contrast, about 13% density change occurs in the case for $Ra = 10^6$ and $\beta\Delta T = 0.33$ due to the large temperature difference between the side walls ($\Delta T = 100$ [K]). This result shows that the change of the fluid density is non-negligible in this case and the compressible fluid model is needed for

Table 2: Comparison of predicted minimum density in steady state

Ra ($\beta\Delta T$)	10^3 (3.33×10^{-3})	10^6 (0.33)
$\rho_{f,\min}/\rho_{f,0}$	0.998	0.864

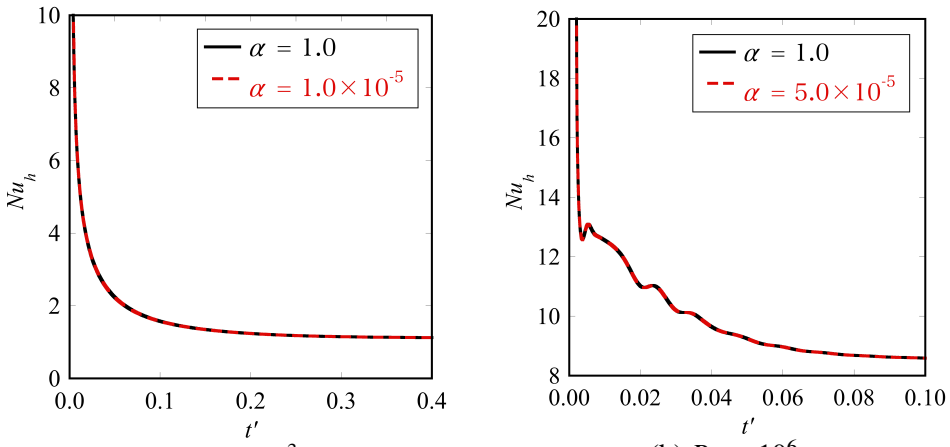

(a) $Ra = 10^3$ (b) $Ra = 10^6$

Figure 4: Time histories of Nu_h

reasonable computations.

Figure 4 shows time histories of the Nusselt number Nu_h on the heated wall under maximum and minimum α conditions. Here, $\alpha = 1.0$ (maximum case) indicates that we do not use the control method for the speed of sound. In addition, Nu_h is defined as follows:

$$Nu_h = -\int_0^1 \left.\frac{\partial \Theta}{\partial X_1}\right|_{X_1=0} dX_2, \tag{26}$$

where Θ, X_1, and X_2 are $\Theta = (T - T_c)/(T_h - T_c)$, $X_1 = x_1/L$, and $X_2 = x_2/L$, respectively. As shown in Fig. 4, the time histories of Nu_h obtained by different α values are in good agreement with each other in both Ra conditions. However, when we use the smaller α values than those given in Table 1, some discrepancies occur in Nu_h and unphysical temperature distributions are predicted. This result shows that 10^{-5} and 5.0×10^{-5} are allowable minimum values of α for $Ra = 10^3$ and 10^6 to obtain reasonable temperature distributions in this application.

Table 3 gives the comparison of Nu_h in the steady state between the proposed fully explicit compressible fluid model, our conventional semi-implicit compressible fluid model [1], and a conventional implicit incompressible fluid model [10]. Here, the incompressible fluid model cannot be applied to the case for $Ra = 10^6$ since $\beta\Delta$ is 0.33 and the density

Table 3: Comparison of Nu_h in steady state

		Fully explicit (present)		Semi-implicit [1]	Barakos [10]
$Ra = 10^3$	α	1.0	1.0×10^{-5}	–	–
($\beta\Delta T << 1$)	Nu_h	1.12	1.12	1.12	1.11
$Ra = 10^6$	α	1.0	5.0×10^{-5}	–	–
($\beta\Delta T = 0.33$)	Nu_h	8.54	8.54	8.53	–

Table 4: Comparison of S_E/S_I

$Ra = 10^3$	α	1.0	0.50	0.10	1.0×10^{-3}	5.0×10^{-5}	1.0×10^{-5}
	S_E/S_I	40.4	27.6	12.2	1.28	0.277	0.128
$Ra = 10^6$	α	1.0	0.50	0.10	1.0×10^{-3}	5.0×10^{-5}	1.0×10^{-5}
	S_E/S_I	21.4	15.5	6.82	0.680	0.156	–

change of the fluid is non-negligible. As shown in Table 3, obtained Nusselt numbers are in good agreement with the reference results regardless of α values. This result shows that discrepancies of predicted temperature distributions are sufficiently small between the proposed fully explicit method and the conventional semi-implicit method. In addition, it is also confirmed that α has negligible effects on the accuracy of the computations within the range of values set in this study.

The comparison of the computational time is given in Table 4. In Table 4, S_E and S_I are elapsed times to obtain results at $t' = 1.0$ by the proposed fully explicit method and our conventional semi-implicit method in which the simultaneous linear equations are solved by the Bi-CGSTAB method [11]. Here, $C_{a,\max}$ obtained by the semi-implicit method is 8.16×10^2 in $Ra = 10^3$ and 8.73×10^2 in $Ra = 10^6$, respectively. As shown in Table 4, S_E decreases when the smaller α is set in the computations since the larger Δt can be adopted by the control method for the speed of sound which improves the CFL condition without solving simultaneous linear equations. As a result, the proposed fully explicit method enables to calculate the natural convection about $6 \sim 8$ times faster than the semi-implicit one by using appropriate α values.

4. Conclusions

In this study, the new fully explicit computational method using the control method for the speed of sound is proposed to calculate non-isothermal and compressible low Mach number gas flows without solving simultaneous linear equations in the pressure calculation stage. As a result of the application to the natural convection in a square cavity, predicted Nusselt numbers are in good agreement with those by the conventional semi-implicit method. In addition, it is also demonstrated that the proposed fully explicit method enables to conduct computations about $6 \sim 8$ times faster than the conventional semi-implicit method by setting the appropriate value of the artificial coefficient for the pressure fluctuation terms.

References

[1] D. Toriu, S. Ushijima: Multiphase computational method for thermal interactions between compressible fluid and arbitrarily shaped solids, *International Journal for Numerical Methods in Fluids*, 87:8 (2018), 383–400.

[2] T. Himeno, T. Watanabe, A. Konno: Numerical analysis for propellant management in rocket tanks, *Journal of Propulsion Power*, 21:1 (2005), 76–86.

[3] E. Turkel: Preconditioned methods for solving the incompressible and low speed compressible equations, *Journal of Computational Physics*, 72:2 (1987), 277–298.

[4] Y. H. Choi, C. L. Merkle: The application of preconditioning in viscous flows, *Journal of Computational Physics*, 105:2 (1993), 207–223.

[5] M. Rempel: Solar differential rotation and meridional flow: the role of a subadiabatic tachocline for the Taylor-Proudman balance, *The Astrophysical Journal*, 622 (2005), 1320–1332.

[6] H. Hotta, M. Rempel, T. Yokoyama, Y. Iida, Y. Fan: Numerical calculation of convection with reduced speed of sound technique, *Astronomy & Astrophysics*, 539 (2012), A30.

[7] C. M. Rhie, W. L. Chow: Numerical study of the turbulent flow past an airfoil with trailing edge separation, *AIAA Journal*, 21 (1983), 1525–1532.

[8] S. Yamamoto, H. Daiguji: Higher-order-accurate upwind schemes for solving the compressible Euler and Navier-Stokes equations, *Computers & Fluids*, 22:2–3 (1993), 259–270.

[9] JSME: *JSME Data Book: Thermophysical Properties of Fluids*, Maruzen, Tokyo, 2014, 162–192. (in Japanese)

[10] G. Barakos, E. Mitsoulis, D. Assimacopoulos: Natural convection flow in a square cavity revisited: laminar and turbulent models with wall functions, *International Journal for Numerical Methods in Fluids*, 18:7 (1994), 695–719.

[11] H. A. van der Vorst: Bi-CGSTAB: A fast and smoothly converging variant of Bi-CG for the solution of nonsymmetric linear systems, *SIAM Journal on Scientific and Statistical Computing*, 13:2 (1992), 631–644.